

# Massive MIMO-NOMA Systems Secrecy in the Presence of Active Eavesdroppers

Marziyeh Soltani<sup>†</sup>, Mahtab Mirmohseni<sup>†</sup>, and Panos Papadimitratos<sup>\*</sup>

<sup>†</sup>Department of Electrical Engineering, Sharif University of Technology, Tehran, Iran

<sup>\*</sup>Networked Systems Security group, KTH Royal Institute of Technology, Stockholm, Sweden

**Abstract**—Non-orthogonal multiple access (NOMA) and massive multiple-input multiple-output (MIMO) systems are highly efficient. Massive MIMO systems are inherently resistant to passive attackers (eavesdroppers), thanks to transmissions directed to the desired users. However, active attackers can transmit a combination of legitimate user pilot signals during the channel estimation phase. This way they can mislead the base station (BS) to rotate the transmission in their direction, and allow them to eavesdrop during the downlink data transmission phase. In this paper, we analyse this vulnerability in an improved system model and stronger adversary assumptions, and investigate how physical layer security can mitigate such attacks and ensure secure (confidential) communication. We derive the secrecy outage probability (SOP) and a lower bound on the ergodic secrecy capacity, using stochastic geometry tools when the number of antennas in the BSs tends to infinity. We adapt the result to evaluate the secrecy performance in massive orthogonal multiple access (OMA). We find that appropriate power allocation allows NOMA to outperform OMA in terms of ergodic secrecy rate and SOP.

**Index Terms**—Massive MIMO, NOMA, Secrecy, Stochastic Geometry.

## I. INTRODUCTION

Massive multiple-input multiple-output (MIMO) is a key technology for 5G networks [1], increasing spectral and energy efficiency, with the help of base stations (BSs) with large antenna arrays supporting many users in the same frequency-time domain [2]. BSs operate in time division duplex (TDD) for the uplink and downlink. For channel estimation, the users transmit orthogonal pilot sequences for the BSs to estimate uplink channels. Exploiting channel reciprocity, BSs also obtain the downlink channel state information (CSI) [3]. The limited number of pilot sequences implies their reuse in different cells and thus inaccurate CSI estimates due to interfering pilot sequences (pilot contamination) [4].

Recently, non-orthogonal multiple access (NOMA) systems have received attention as they improve energy and spectral efficiency [5]. NOMA separates users in the power domain and allows operating simultaneously in the same frequency, by exploiting superposition coding at the transmitter and successive interference cancellation (SIC) at the receivers [6]. Combining the advantages of massive MIMO and NOMA is being investigated [7], [8]. For a large number of users in each cell, clustering users with the same pilot sequence is beneficial: with a limited number of orthogonal pilot sequences, the residual interference after imperfect SIC is reduced. However, user clustering (and use of the same pilot) degrades the uplink

training, decreasing spatial resolution, because of intra-cluster pilot interference.

Experience teaches that security for such emerging wireless networks is important, notably to safeguard data secrecy. Without resorting to cryptographic approaches, physical layer security (PLS) can guarantee secure communication, that is, preserve confidentiality, in massive MIMO-NOMA networks. Interestingly, massive MIMO is inherently secure against passive eavesdroppers, thanks to large antenna arrays and directed beams to intended users.

However, these systems are vulnerable to active attacks, notably when attackers send the same pilot sequences as legitimate users during the channel estimation phase [9]. The result is that the BS directed beam is rotated towards the attacker that eavesdrops data transmission. This active attack can be seen as pilot contamination; however, approaches to mitigate non-malicious pilot contamination in multi-cell scenarios, such as blind CSI estimation and protocol-based methods [10], can be of limited use against deliberate contamination, against adversaries; at unknown distances, injecting arbitrarily pilot sequences [11]. Active attackers in each cluster, a single-cell massive MIMO-NOMA network, were considered in [8]: a closed-form expression for the ergodic secrecy rate was derived (considering the randomness of channel coefficients, relying on PLS). It is more realistic to study a multi-cell network with randomly located BSs and multiple randomly located attackers. To the best of our knowledge, the secrecy outage probability (SOP) and the ergodic secrecy rate for multi-cell massive MIMO-NOMA systems have not been derived for the random location of nodes.

In this paper, we investigate the secrecy performance of PLS approaches in a multi-cell massive MIMO-NOMA network; with BSs, attackers, and users are distributed according to independent homogeneous Poisson point processes (HPPPs). The attackers can eavesdrop downlink data transmissions after interfering with the channel estimation phase (sending a combination of pilot sequences). We consider the effects of path loss and Rayleigh fading and rely on a two-user NOMA scheme, i.e., two users in each cluster. This differs significantly from prior art, which considers the randomness of channel coefficients in a single cell [8]; in our model, all nodes are randomly distributed. We derive secrecy outage probability (SOP) and a lower bound on the ergodic secrecy capacity.

To achieve this, we address a set of challenges. First, the attacker-sent pilot sequences, during the channel estimation

phase, same as those sent by legitimate users, affect the resultant estimated channel vector for each user. Second, due to NOMA, the distances between users and BSs are correlated for any two users in a cluster. The statistical properties of the inter-cell pilot contamination interference affect both attackers and legitimate user ergodic rates. Last but not least, the extent of information leakage to the adversary is influenced by the random attacker and BS locations, which must be considered in its derivation approach.

In summary, our contributions are:

- 1) A connection-level analysis and the resultant; asymptotic expressions of signal-to-noise and interference ratio (SINR) at legitimate users and attackers, when the number of BS antennas tends to infinity (massive MIMO scenario). We consider imperfect channel estimation in a worst-case adversarial scenario (in other words, the strongest attacker).
- 2) An analysis of the system secrecy performance through the derivation of the ergodic secrecy rate and SOP for any desired pair of users. Each user connects to its nearest BS and each BS chooses a fixed number of users in its Voronoi cell to serve. We use the Alzer inequality [12, Appendix A] for a tight approximation of the cumulative distribution function (CDF) of interference caused by pilot contamination.
- 3) Simulation results that confirm the analysis. For comparison, after adapting our results to a massive MIMO-orthogonal multiple access (OMA) network, by allocating the total power, both for channel estimation and downlink communication, to a single user: our results show that NOMA gains in massive MIMO systems necessitate appropriate power allocation for NOMA users.

In the rest of the paper, Section II discusses the related works and Section III describes the system model, including the attackers. Section IV details the transmission strategy. In Sections V and VI, we characterize the ergodic secrecy rate and SOP of the system, respectively. Our simulation results are provided in Section VII, before we conclude.

## II. RELATED WORKS

The secrecy performance of NOMA systems was studied both with random channels and the random location of the users. In [13], a closed-form solution for maximizing the secrecy rate was calculated in a single-cell downlink NOMA network in the presence of a passive eavesdropper, with no randomness for channel vectors or node locations considered. In [14], for the same type of network, users were uniformly distributed in a disk around the BS and eavesdroppers were distributed according to an HPPP. Exact expressions for SOP for single- and multiple-antenna scenarios were obtained. A downlink NOMA network with two users was considered in [15], with an external passive eavesdropper and all nodes with a single-antenna; the SOP and the ergodic secrecy rate were derived in closed form, by considering the channel coefficients randomness.

In the presence of active attackers, the secrecy performance of massive MIMO networks was studied in [11], [16], [17]. In [16], a self-contamination technique was proposed: a BS can detect the attacker by sending a random signal and superimposing it on its pilot sequences. In [11], for a single-cell massive MIMO system, the attackers sought to minimize the sum rate of downlink transmissions, knowing the locations of BS and users precisely or probabilistically. In [17], for a multi-cell massive MIMO system with fixed-location users, in the presence of a multi-antenna attacker, an asymptotic achievable secrecy rate was derived when the number of BS antennas approaches infinity.

The combination of massive MIMO and NOMA techniques was studied for different scenarios. In [7], fully non-orthogonal communication for massive access, consisting of non-orthogonal channel estimation and NOMA, was designed; considering the randomness of channel coefficients, a tight lower bound on the spectral efficiency was derived. In [18], for a massive MIMO-NOMA network, the achievable rate of a typical user, for randomly located users and BSs, was obtained with imperfect SIC. In [19], in a single-cell downlink massive MIMO-NOMA system, the outage probability and the bit error rate were derived, with the help of random matrix theory. In [8], for a single-cell massive MIMO-NOMA network with an active attacker in each cluster, with randomness in channel coefficients, a closed-form expression for the ergodic secrecy rate was derived.

**Comparison to our work:** The most relevant works are [18] and [8]. Compared to [18], beyond the secrecy constraint, our work differs in terms of ordering the NOMA users in each cluster, calculating both ergodic secrecy rate and SOP, and in terms of the statistical properties calculation for the pilot contamination interference term. Moreover, unlike [8] that derives the ergodic secrecy rate in a single-cell system with random channel vectors, we derive the SOP and the ergodic secrecy rate, considering randomness of both channel vectors and user locations in a multi-cell system.

## III. SYSTEM MODEL

**Notation:** Bold letters denote vectors.  $P(\cdot)$ ,  $f_x(\cdot)$ ,  $F_x(\cdot)$ ,  $E[\cdot]$  represent the probability, the probability density function (PDF), the cumulative distribution function (CDF), and the expectation, respectively.  $\mathbf{X}^T$ ,  $\mathbf{X}^H$  and  $\mathbf{X}^*$  are the transpose, the Hermitian transpose and the conjugate of  $\mathbf{X}$ , respectively.  $\mathbf{I}_M$  is an  $M \times M$  identity matrix. The Euclidean norm is  $\|\cdot\|$  and  $\mathcal{CN}(\cdot, \cdot)$ ; denotes a multi-variate circularly-symmetric complex Gaussian distribution;  $\mathbb{C}$  and  $\mathbb{N}$  are sets of complex and natural numbers.

We consider a NOMA-enabled massive MIMO system in time-division duplex (TDD) mode and downlink transmission. In TDD mode, there are two phases for downlink transmission during a coherence time interval: pilot transmission (channel estimation) and downlink data transmission. First, users transmit their pilot sequences and the BS estimates the channel coefficient vectors for its serving users. Then, based on these estimates, the BS calculates the precoding vectors for each

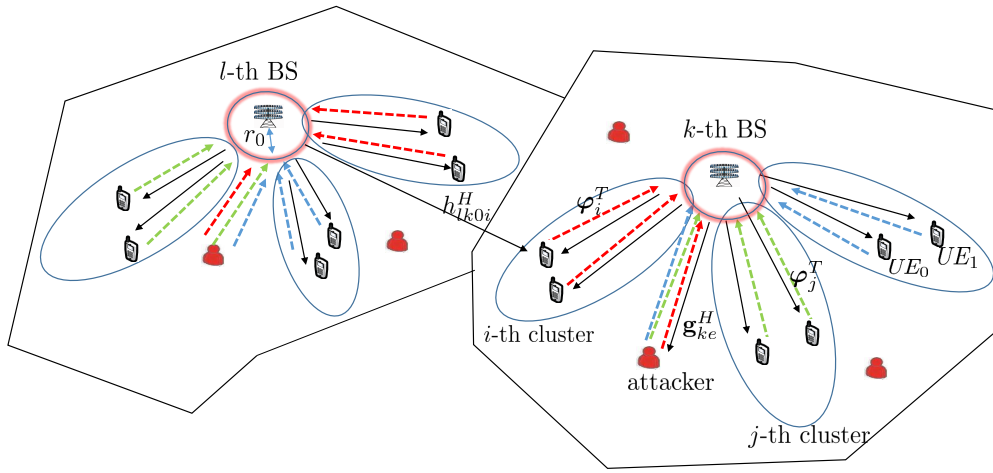


Fig. 1. System model: dashed and solid lines are used to show the pilot and data transmission phases, respectively.

user and uses those vectors during the downlink transmission of data to the users. We assume there is one BS in each cell, with an array of  $M$  antennas. BSs are distributed according to an homogeneous Poisson point processes (HPPP),  $\Phi_b$ , with density  $\lambda_b$ . The system model is illustrated in Fig. 1.

#### A. Legitimate users

Single-antenna users are distributed according to an HPPP with density  $\lambda_u$ , which, we assume, is much greater than  $\lambda_b$ . In fact, we consider a full-load scenario with many users in the cell of each BS. Each user wishes to connect to its nearest BS. The BS selects  $N_u$  users and serves them. We employ two-user NOMA<sup>1</sup>, thus the  $N_u$  users in a cell serviced by one BS are organized into  $I = \frac{N_u}{2}$  clusters.

For the first cluster, the BS selects two random users and labels them as cluster 1; the first pilot sequence in the pilot codebook is assigned to these two users. For the second cluster, the BS randomly selects two other users, different from the ones in cluster 1, and allocates the second pilot sequence in the codebook. The BS performs this procedure until  $I$  clusters are formed. We assume that the number of users is very high, thus selecting two users at each stage does not affect the distribution of the rest remaining users. Distinct, orthogonal pilot sequences are assigned to each cluster in a cell, while within a cluster users have the same pilot sequence. If  $\varphi_i$  is the pilot sequence assigned to cluster  $i$  and  $\varphi_j$  to cluster  $j$ , then we have:

$$\varphi_i^H \varphi_j = \begin{cases} 1 & i = j \\ 0 & \text{otherwise} \end{cases}, \quad (1)$$

where  $\varphi$  is a  $q \times 1$  vector. The same cluster-pilot mapping is used for all cells. As the maximum number of mutually orthogonal sequences of length  $q$  is equal to  $q$ , the number of clusters in each cell,  $I$ , must not be greater than  $q$ , to guarantee orthogonality.

<sup>1</sup>Our results can be extended to  $m$ -user NOMA but for simplicity, we assume two-user NOMA.

**Channel:** We consider the effects of both small-scale fading and the large-scale path loss effects. The latter depends on the distance between the transmitter and the receiver, while small-scale fading is a complex-Gaussian distributed random variable. The channel vector between the  $m$ -th user in the  $i$ -th cluster of the  $l$ -th cell and the BS in the  $k$ -th cell is denoted by:

$$\mathbf{h}_{klmi} r_{klmi}^{-\alpha/2}, \quad \mathbf{h}_{klmi} \sim \mathcal{CN}(\mathbf{0}, \mathbf{I}_M), \quad (2)$$

for  $m \in \{0, 1\}$ ,  $i \in \{1, \dots, I\}$ ,  $k, l \in \mathbb{N}$ , and  $\mathbf{h}_{klmi} \in \mathbb{C}^{M \times 1}$  the small-scale fading coefficient,  $r_{klmi}$  the distance between the mentioned user and the  $k$ -th BS, and  $\alpha$  the path loss exponent. In fact, we assume that the channel model is *uncorrelated Rayleigh fading* and has no dominant spatial directivity [20]. According to the law of large numbers, we have:

$$\frac{\mathbf{h}_{klmi}^H \mathbf{h}_{\hat{k}\hat{l}\hat{m}\hat{i}}}{M} \xrightarrow{M \rightarrow \infty} \begin{cases} 1 & k = \hat{k}, l = \hat{l}, m = \hat{m}, i = \hat{i} \\ 0 & \text{otherwise} \end{cases}. \quad (3)$$

#### B. Illegitimate users (attackers)

There are many single-antenna attackers in each cell, distributed outside the eavesdropper-free region (a disk of radius  $r_0$  around BS), according to an HPPP,  $\Phi_e$ , of density  $\lambda_e$ . We assume that all attackers know the pilot codebook and send a combination of all pilot sequences during the channel estimation phase. As a result, during the downlink transmission, they can eavesdrop data intended for any user in any cluster. We investigate the worst case by considering an attacker that has maximum SINR.

**Channel:** The channel vector between the  $k$ -th BS and an arbitrary attacker is denoted by:

$$\mathbf{g}_{ke} r_{ke}^{-\alpha/2}, \quad \mathbf{g}_{ke} \sim \mathcal{CN}(\mathbf{0}, \mathbf{I}_M), \quad (4)$$

$\mathbf{g}_{ke} \in \mathbb{C}^{M \times 1}$  is the small-scale fading coefficient and  $r_{ke}$  is the distance between the attacker and the  $k$ -th BS. According to the law of large numbers,  $\mathbf{h}_{klmi}^H \mathbf{g}_{ke} / M$  tends to 1, in probability as  $M$  goes to  $\infty$ , only when the attacker and the legitimate

user are at the same location, for  $m \in \{0, 1\}$ ,  $i \in \{1, \dots, I\}$ ,  $k, l$ ,  $\hat{k} \in \mathbb{N}$ ; this occurs with zero probability. Otherwise  $\mathbf{h}_{klmi}^H \mathbf{g}_{\hat{k}e} / M$  tends to zero. Similarly, for two illegitimate channel vectors, in probability, we have:

$$\frac{\mathbf{g}_{ke}^H \mathbf{g}_{\hat{k}e}}{M} \stackrel{M \rightarrow \infty}{=} \begin{cases} 1 & k = \hat{k}, e = \tilde{e} \\ 0 & \text{otherwise} \end{cases}. \quad (5)$$

#### IV. TRANSMISSION STRATEGY

##### A. Channel Estimation Phase

Each BS needs an estimates downlink channel vectors to design precoding vectors for the data transmission phase. Users in cluster  $i$  send pilot  $\boldsymbol{\varphi}_i^T$ , with  $b_i$  the power allocation coefficient each user allocates to  $\boldsymbol{\varphi}_i$ .  $P_p$  is the maximum transmission power for each users and attacker. Each attacker sends  $\sum_{i=1}^I \sqrt{d_i P_p} \boldsymbol{\varphi}_i^T$ , in which  $d_i$  is the power allocation coefficient for the  $i$ -th pilot sequence. The received signal at the end of the pilot transmission phase at the  $k$ -th BS is:

$$\begin{aligned} \mathbf{y}_k &= \sum_{m=0}^1 \sum_{i=1}^I \sum_{l=1}^{\infty} \mathbf{h}_{klmi} r_{klmi}^{-\alpha/2} \boldsymbol{\varphi}_i^T \sqrt{b_m P_p} \\ &+ \sum_{e \in \Phi_e} \mathbf{g}_{ke} r_{ke}^{-\alpha/2} \left( \sum_{i=1}^I \sqrt{d_i P_p} \boldsymbol{\varphi}_i^T \right) + \mathbf{W}_k, \end{aligned} \quad (6)$$

where  $m$ ,  $i$  and  $l$  denote, respectively, the  $m$ -th user in the  $i$ -th cluster of the  $l$ -th cell;  $\mathbf{W}_k^{M \times q}$  is the noise component at the  $k$ -th BS with i.i.d elements drawn according to a distribution  $\mathcal{CN}(0, \sigma^2)$ . In (6), the first term denotes the pilot sequences sent by all legitimate users and the second term denotes the pilot sequences sent by the attackers. To estimate the channel vector of a legitimate user, the BS multiplies the received signal,  $\mathbf{y}_k$ , with the user pilot sequence. This eliminates the effect of the other pilot sequences that are by design orthogonal. However, the effect of the pilot sequences sent by the users in the same cluster as the mentioned user remains. The effect of the adversarial transmission remains too, as it was a combination of all pilot sequences.

By defining  $\mathcal{B} = \{(\hat{m}, l) | \hat{m} \in \{0, 1\}, l \in \mathbb{N}\}$ , the estimation of the channel vector for the  $m$ -th user in the  $\tilde{i}$ -th cluster in the  $k$ -th cell, calculated at the  $k$ -th BS, is:

$$\begin{aligned} \hat{\mathbf{h}}_{kkmi} &\stackrel{(a)}{=} \frac{\mathbf{y}_k \boldsymbol{\varphi}_i^*}{\sqrt{b_m P_p}} \\ &\stackrel{(b)}{=} \mathbf{h}_{kkmi} r_{kkmi}^{-\alpha/2} + \sum_{\mathcal{B} \setminus \{\hat{m}=m, l=k\}} \frac{\mathbf{h}_{kl\hat{m}\tilde{i}} r_{kl\hat{m}\tilde{i}}^{-\alpha/2} \sqrt{b_{\hat{m}}}}{\sqrt{b_m}} \\ &+ \sum_{e \in \Phi_e} \frac{\mathbf{g}_{ke} r_{ke}^{-\alpha/2} \sqrt{d_{\tilde{i}}}}{\sqrt{b_m}} + \frac{\mathbf{W}_k \boldsymbol{\varphi}_i^*}{\sqrt{b_m P_p}}, \end{aligned} \quad (7)$$

where (a) follows from the estimation method (described above) and (b) follows from (1) and (6).

##### B. Downlink Data Transmission Phase

For the preorder design, in massive MIMO systems, linear precoding is nearly optimal [21]; we use here one such scheme, matched filter precoding. We use different precoding

vectors for each user in a cluster, based on their estimated channels. The  $l$ -th BS multiplies the intended data for user  $m$  in the  $i$ -th cluster of the  $l$ -th cell by  $\hat{\mathbf{h}}_{llmi}$ . We assume that users in  $i$ -th cluster of  $k$ -th cell,  $i \in \{1, \dots, I\}$ ,  $k \in \mathbb{N}$ , are ordered based on descending  $S_m = r_{kkmi}^{-2\alpha} / \sum_{l \neq k} r_{lkm}^{-2\alpha}$  ( $m \in \{0, 1\}$ ) values. We remark that ordering method results in larger intra-cell interference in comparison with ordering the users only based on their distance to serving BSs.

Throughout this paper, in each cluster, we term a user *central* if it has  $\max(S_0, S_1)$ , not necessarily the closest to the serving BS. The other user is termed, simply, the *second* user. In equations,  $m = 0$  denotes the central user and  $m = 1$  denotes the second user. NOMA allows the central user to decode the signal of the second user, cancel it from the received signal, and then decode its own signal. The second user decodes its own signal by treating the central user's signal as noise. The power coefficient allocated to user  $m$  for downlink transmission is  $a_m$ ; thus,  $a_0 + a_1 = 1$ . NOMA mandates that; more power must be allocated to the second user, i.e.,  $a_0 < a_1$ . BS allocates power  $P_d a_m$  to user  $m$ . The transmitted power is normalized by  $2M$  (number of users in each cluster multiplied by the number of BS antennas).  $s_{lmi}$  is the data the  $l$ -th BS sends to user  $m$  in the  $i$ -th cluster of the  $l$ -th cell, with  $\|s_{lmi}\| = 1$ .  $w_d$  is scalar additive white Gaussian noise with variance  $\sigma_n^2$ .  $\mathbf{x}_l^{M \times 1}$  the signal transmitted by the  $l$ -th BS is:

$$\mathbf{x}_l = \sum_{i=1}^I \sum_{m=0}^1 \hat{\mathbf{h}}_{llmi} s_{lmi} \sqrt{\frac{P_d a_m}{2M}}. \quad (8)$$

Now, we derive the received signal at an arbitrary legitimate user.  $\mathbf{h}_l$  is the channel coefficient and  $r_l$  is distance between the user and the  $l$ -th BS. The received signal at the legitimate user is:

$$y = \sum_{l=1}^{\infty} \mathbf{h}_l^H r_l^{-\alpha/2} \mathbf{x}_l + w_d. \quad (9)$$

1) *Received signal at the legitimate user:* By substituting (7) and (8) into (9) and by defining  $\hat{\mathcal{B}} = \{(s, t) | s \in \{0, 1\}, t \in \mathbb{N}\}$ , the received signal at the central user in the  $\tilde{i}$ -th cluster of the  $k$ -th cell is calculated by replacing  $y$ ,  $\mathbf{h}_l$  and  $r_l$  with  $y_{k0\tilde{i}}$ ,  $\mathbf{h}_{lk0\tilde{i}}$  and  $r_{lk0\tilde{i}}$ :

$$\begin{aligned} y_{k0\tilde{i}} &= \sum_{l=1}^{\infty} \mathbf{h}_{lk0\tilde{i}}^H r_{lk0\tilde{i}}^{-\alpha/2} \sum_{i=1}^I \sum_{m=0}^1 s_{lmi} \sqrt{\frac{P_d a_m}{2M}} (\mathbf{h}_{llmi} r_{llmi}^{-\alpha/2} \\ &+ \sum_{\hat{\mathcal{B}} \setminus \{s=m, t=l\}} \frac{\mathbf{h}_{ltsi} r_{ltsi}^{-\alpha/2} \sqrt{b_s}}{\sqrt{b_m}} \\ &+ \sum_{e \in \Phi_e} \frac{\mathbf{g}_{le} r_{le}^{-\alpha/2} \sqrt{d_{\tilde{i}}}}{\sqrt{b_m}} + \frac{\mathbf{W}_l \boldsymbol{\varphi}_i^*}{\sqrt{b_m P_p}}) + w_d. \end{aligned} \quad (10)$$

Similarly, the received signal at the second user in the  $\tilde{i}$ -th cluster of the  $k$ -th cell is denoted as  $y_{k1\tilde{i}}$  and can be calculated by substituting (7) and (8) into (9) and replacing  $y$ ,  $\mathbf{h}_l$  and  $r_l$  with  $y_{k1\tilde{i}}$ ,  $\mathbf{h}_{lk1\tilde{i}}$  and  $r_{lk1\tilde{i}}$ , respectively.

Now, to derive the achievable secrecy rates, we have to calculate  $\text{SINR}_{k0\tilde{i}}^{w_0}$ , the SINR of the central user (in the  $\tilde{i}$ -th cluster of  $k$ -th cell) when decoding its own message ( $w_0$ ) after omitting the second user's message ( $w_1$ );  $\text{SINR}_{k0\tilde{i}}^{w_1}$ , the SINR of the central user when decoding the second user signal; and  $\text{SINR}_{k1\tilde{i}}^{w_1}$ , the SINR of the second user (in  $\tilde{i}$ -th cluster of  $k$ -th cell) when decoding its own signal.

**Lemma 1:**

$$\text{SINR}_{k0\tilde{i}}^{w_0} = \frac{a_0 r_{kk0\tilde{i}}^{-2\alpha}}{R b_0 \sum_{l \neq k} r_{lk0\tilde{i}}^{-2\alpha}}, \quad (11)$$

$$\text{SINR}_{k0\tilde{i}}^{w_1} = \frac{\frac{b_0 a_1 r_{kk0\tilde{i}}^{-2\alpha}}{b_1}}{R b_0 \sum_{l \neq k} r_{lk0\tilde{i}}^{-2\alpha} + a_0 r_{kk0\tilde{i}}^{-2\alpha}}, \quad (12)$$

$$\text{SINR}_{k1\tilde{i}}^{w_1} = \frac{a_1 r_{kk1\tilde{i}}^{-2\alpha}}{\frac{a_0 b_1 r_{kk1\tilde{i}}^{-2\alpha}}{b_0} + R b_1 \sum_{l \neq k} r_{lk1\tilde{i}}^{-2\alpha}}. \quad (13)$$

*Proof:* Please see Appendix A. ■

2) *Received signal at the attacker:* The attacker acts as a jammer during the pilot phase and as an eavesdropper during the downlink data transmission phase. The signal received at an arbitrary attacker,  $\tilde{e}$ , can be calculated by substituting (7) and (8) into (9), and by replacing  $y$ ,  $\mathbf{h}_l$  and  $r_l$  with  $y_{\tilde{e}}$ ,  $\mathbf{g}_{l\tilde{e}}^H$  and  $r_{l\tilde{e}}$ :

$$\begin{aligned} y_{\tilde{e}} &= \sum_{l=1}^{\infty} r_{l\tilde{e}}^{-\alpha/2} \sum_{i=1}^I \sum_{m=0}^1 s_{lmi} \sqrt{\frac{P_d a_m}{2M}} (\mathbf{g}_{l\tilde{e}}^H \mathbf{h}_{lmi} r_{lmi}^{-\alpha/2}) \\ &+ \sum_{\tilde{\mathcal{B}} \setminus \{s=m, t=l\}} \frac{\mathbf{g}_{l\tilde{e}}^H \mathbf{h}_{ltsi} r_{ltsi}^{-\alpha/2} \sqrt{b_s}}{\sqrt{b_m}} \\ &+ \sum_{e \in \Phi_e} \frac{\mathbf{g}_{l\tilde{e}}^H \mathbf{g}_{le} r_{le}^{-\alpha/2} \sqrt{d_i}}{\sqrt{b_m}} + \frac{\mathbf{g}_{l\tilde{e}}^H \mathbf{W}_l \varphi_i^*}{\sqrt{b_m P_p}} + w_e. \end{aligned} \quad (14)$$

The attacker experiences the same noise power as the legitimate users. Now, we let  $M \rightarrow \infty$ , we use (3) and (5), and we assume that the attacker wants to eavesdrop the message of the central user. Based on the approach in Appendix A, noting  $\sum_{i=1}^I d_i = 1$  and ignoring  $\sigma_n^2$ , the SINR of the attacker eavesdropping,  $w_0$ , the message to the central user, is:

$$\text{SINR}_{\tilde{e}}^{w_0} = \frac{\frac{d_i a_0 r_{k\tilde{e}}^{-2\alpha}}{b_0}}{r_{k\tilde{e}}^{-2\alpha} (R - \frac{d_i a_0}{b_0}) + R \sum_{l \neq k} r_{l\tilde{e}}^{-2\alpha}}. \quad (15)$$

We remark that unlike the central user, the attacker cannot perform SIC, thus being subject to comparatively increased interference. Moreover, from (15), it is clear that if the attacker had not sent its pilot sequence during the channel estimation phase (i.e.,  $d_i = 0$ ), it would not have received any information, due to the massive MIMO directed beam. If the attacker intends to eavesdrop the second user message ( $w_1$ ), its SINR is derived similarly:

$$\text{SINR}_{\tilde{e}}^{w_1} = \frac{\frac{d_i a_1 r_{k\tilde{e}}^{-2\alpha}}{b_1}}{r_{k\tilde{e}}^{-2\alpha} (R - \frac{d_i a_1}{b_1}) + R \sum_{l \neq k} r_{l\tilde{e}}^{-2\alpha}}. \quad (16)$$

## V. ERGODIC SECRECY RATE

We calculate a lower bound on the ergodic secrecy rate for our system model (Section III). The ergodic secrecy rate of a legitimate user can be computed as:

$$C_s = E[(R_{\text{user}} - R_{\text{eavs}})^+], \quad (17)$$

where  $(x)^+ = \max(0, x)$  and  $R_{\text{user}}$  and  $R_{\text{eavs}}$  are the rates of the legitimate user channel and the attacker, eavesdropper during downlink, respectively. As the BS is equipped with a massive number of antennas, the ergodic secrecy rate is lower-bounded by [22]:

$$C_s = (E[R_{\text{user}}] - E[R_{\text{eavs}}])^+. \quad (18)$$

We compute the achievable rates for the legitimate and the eavesdropper channels separately, to obtain a lower bound on the secrecy ergodic rate. We define:

$$\begin{aligned} \tilde{F}(\tilde{f}) &\triangleq \int_0^{\infty} \sum_{n=1}^N (-1)^{n+1} \binom{N}{n} e^{\int_r [\exp(-R\tilde{f}\eta nr^{2\alpha} x^{-2\alpha}) - 1] 2\pi\lambda_b x dx} \\ &2\pi\lambda_b r e^{-\lambda_b \pi r^2} dr, \end{aligned} \quad (19)$$

$$\begin{aligned} V(v, \tilde{v}) &\triangleq \exp(-2\pi\lambda_b \int_{r_0}^{\infty} (1 - e^{-v u \tilde{\eta} \frac{R \tilde{v} s^{-2\alpha} r^{2\alpha}}{d_i}}) s ds) \\ &e^{-v u \tilde{\eta} (\frac{R \tilde{v}}{d_i} - 1)}, \end{aligned} \quad (20)$$

that is, the ergodic rate of legitimate users and the leakage to the attacker (eavesdropper) and we characterize them in the following lemmas.

**Lemma 2:** The ergodic rate of the central and the second users in the  $\tilde{i}$ -th cluster of  $k$ -th cell are denoted by  $R_0$  and  $R_1$ , respectively, and are obtained as:

$$R_0 = \int_0^{\infty} (1 - (1 - \tilde{F}(\frac{(2^t - 1)b_0}{a_0}))^2) dt. \quad (21)$$

$$R_1 = \int_0^{\log(1 + \frac{a_1 b_0}{b_1 a_0})} (\tilde{F}(\frac{(2^t - 1)b_1}{a_1 - \frac{(2^t - 1)a_0 b_1}{b_0}}))^2 dt. \quad (22)$$

Where  $\tilde{F}$  is defined in (19).

*Proof:* Please see Appendix B. ■

**Lemma 3:** The ergodic leakage rate to the attacker that seeks to eavesdrop data of the central user in the  $\tilde{i}$ -th cluster of  $k$ -th cell is derived as (23), with  $V$  defined in (20).

*Proof:* Please see Appendix C. ■

A lower bound on the secrecy ergodic rate of the central user can be computed by using (23) and (21). Similarly, the ergodic leakage rate to the attacker seeking to eavesdrop the second user data is obtained by replacing  $a_0$  and  $b_0$  with  $a_1$  and  $b_1$  in (23).

## VI. SECRECY OUTAGE PROBABILITY

We calculate the SOP for both users in the  $\tilde{i}$ -th cluster of the  $k$ -th cell. We define  $\tilde{R}_0$  and  $\tilde{R}_1$  as the targeted data rates for the central and second users, respectively. The SOP event is defined as:

$$\text{SOP} = 1 - P(E_{01} \cap E_{00} \cap E_{11}), \quad (24)$$

$$R_e^0 = \frac{1}{\ln 2} \int_0^\infty \frac{1 - \exp(-2\pi\lambda_e \int_{r_0}^\infty (1 - (\sum_{u=0}^U (-1)^u \binom{U}{u} V(x, \frac{b_0}{a_0}))) r dr)}{1+x} dx. \quad (23)$$

where:  $\bar{E}_{01}$  is the event when the central user cannot decode the second user message,  $w_1$ ;  $\bar{E}_{00}$  is the event when the central user cannot decode its own message,  $w_0$ ; and  $\bar{E}_{11}$  is the event when the second user cannot decode its own message,  $w_1$ . These are, computed as follows:

$$\bar{E}_{01} = \{\log(1 + \text{SINR}_{k0\tilde{i}}^{w_1}) - \log(1 + \text{SINR}_{\tilde{e}}^{w_1}) < \tilde{R}_1\}, \quad (25)$$

$$\bar{E}_{00} = \{\log(1 + \text{SINR}_{k0\tilde{i}}^{w_0}) - \log(1 + \text{SINR}_{\tilde{e}}^{w_0}) < \tilde{R}_0\}, \quad (26)$$

$$\bar{E}_{11} = \{\log(1 + \text{SINR}_{k1\tilde{i}}^{w_1}) - \log(1 + \text{SINR}_{\tilde{e}}^{w_1}) < \tilde{R}_1\}. \quad (27)$$

According to (12), (13) and due to our assumption on user ordered based on  $S_i$ : if  $1 + \text{SINR}_{k1\tilde{i}}^{w_1} > 2^{\tilde{R}_1} (1 + \text{SINR}_{\tilde{e}}^{w_1})$ , then  $1 + \text{SINR}_{k0\tilde{i}}^{w_1} > 2^{\tilde{R}_1} (1 + \text{SINR}_{\tilde{e}}^{w_1})$ , which means:

$$E_{01} \subseteq E_{11}. \quad (28)$$

Thus, the SOP is:

$$\text{SOP} = 1 - (1 - P_{\text{out}}^{w_0})(1 - P_{\text{out}}^{w_1}), \quad (29)$$

where  $P_{\text{out}}^{w_0}$  and  $P_{\text{out}}^{w_1}$  stands for  $P(\bar{E}_{00})$  and  $P(\bar{E}_{11})$ , the outage probabilities of the central user and the second user, respectively. Lemma 4 calculates these probabilities.

**Lemma 4:**  $P_{\text{out}}^{w_0}$  and  $P_{\text{out}}^{w_1}$  are shown at (30) and (31), at the top of the next page, where  $\tilde{F}$ ,  $V$  and  $\tilde{\eta}$  are defined in (19), (20) and Appendix C, respectively.

*Proof:* Please see Appendix D. ■

## VII. SIMULATION RESULTS

We provide numerical results to investigate the SOP and secrecy ergodic rate as a function of system parameters. We validate our analytic results with the help of Monte-Carlo simulations. We also compare the secrecy performance of a massive MIMO-NOMA system with that of a massive MIMO-OMA; we focus on time division multiple access (TDMA), where each of the two users in the cluster is served half of the time. The SINR for an OMA user can be calculated similarly to the derivation of (11), by substituting  $a_1, b_1 = 0, a_0, b_0 = 1$ ; (i.e., by allocating all power to one user). Thus, the SINR of the  $i$ -th user in  $\tilde{i}$ -th cluster of the  $k$ -th cell is:  $\frac{r^{-2\alpha}}{\sum_{l \neq k} r_{lk\tilde{i}}^{-2\alpha}}$ . The ergodic rate for each user can be calculated similar to the derivation of (21) and (22). The ergodic rate of the  $i$ -th user is  $\frac{1}{2} \int_0^\infty (1 - F_{S_i}(2t - 1)) dt$ , with  $F_{S_i}(\cdot)$  defined using (44) and (37). The factor  $\frac{1}{2}$  is needed because only each user in a cluster is served half of the time. The leakage to the strongest eavesdropper and SOP can be obtained similarly to the derivation of (23), (30) and (31), by substituting the above-mentioned changes and by replacing  $\tilde{R}_0$  and  $\tilde{R}_1$  with  $2\tilde{R}_0$  and  $2\tilde{R}_1$ ; respectively.

The simulation results are obtained based on 1000 randomly seeded realizations of the channel and node locations. In each

iteration, we generate a Poisson point process (PPP) with density  $\lambda_b$  in a square region with area  $3km \times 3km$  for BSs locations. We assume each cell has five clusters ( $I = 5$ ). For the user locations, we generate a PPP with high density. Each user is assigned to its nearest BS and each BS randomly selects two of these users to form cluster 1, two other users to form cluster 2 and continues until  $I$  clusters are formed, and it ignores the remaining users. For attackers, we generate a PPP with density  $\lambda_e$  and remove those attacker with distance from any BS less than  $r_0$ . We consider  $N = U = 7$  in plotting the analytic results (defined in (41) and (48))<sup>2</sup>. Our parameters are  $\alpha = 4, b_0 = 0.4, b_1 = 0.6, d_{\tilde{i}} = 0.2, a_0 = 0.4, a_1 = 0.6$  and  $r_0 = 6m$  unless stated otherwise.

Fig. 2 shows the ergodic secrecy rate versus the BS density, for two different attackers densities.  $UE_0, UE_1$ , and Sum, denote the central user, second user, and sum of the ergodic secrecy rates for both users in the cluster, respectively. We see that the simulation results confirm the analytic results. With increasing  $\lambda_b$ , the ergodic secrecy rate increases for both massive MIMO-NOMA and OMA networks; at a higher rate for the massive MIMO-NOMA. This is because users-BS distances decrease: denser networks increase interference from other BSs, but the increase in the desired signal power is higher. Another observation: the secrecy rate for the central user is much higher than that for the second user. This is because the central user has better channel conditions compared to the second user; it performs SIC, while the second user suffers from the central user interference. As expected, increased attacker density implies low secrecy rate, because the SINR for the best positioned attacker is increased. It is noticeable that the secrecy rate is improved by using NOMA in massive MIMO systems.

Fig. 3 shows the ergodic secrecy rate versus the power allocation coefficient for the second user, for different eavesdropper-free zone radii. We use  $\lambda_e = -10dB$  and  $\lambda_b = -35dB$ . Because of the NOMA protocol,  $a_1 > a_0$ ; thus the  $x$ -axis starts at 0.5. By increasing the power ratio for the second user, its secrecy rate increases and it enjoys a fairer share of the rate. This, however, causes a reduction in the central user secrecy rate. As this the central user secrecy rate reduction is higher than the increase of the second user rate, the secrecy sum-rate is reduced. For most of the  $a_1$  values, the sum of secrecy rates for massive NOMA users is higher than that for massive OMA. However, there exists a threshold for power allocation, above which the beneficial effect of NOMA in massive MIMO vanishes (with traditional OMA enjoying a larger secrecy sum rate). Another observation is that by increasing the size of the eavesdropper-free area around the BSs,

<sup>2</sup>We observe that a larger  $U$  or  $N$  values do not change the results.

$$P_{\text{out}}^{w_0} = \int_0^\infty (1 - 2\tilde{F}(\frac{(2^{\tilde{R}_0}(1+z)-1)b_0}{a_0}) + (\tilde{F}(\frac{(2^{\tilde{R}_0}(1+z)-1)b_0}{a_0}))^2)(-2\pi\lambda_e(\int_{r_0}^\infty r dr(-\sum_{u=0}^U (-1)^u \binom{U}{u})(-u\tilde{\eta}(\frac{Rb_0}{a_0 d_{\tilde{i}}}-1) - 2\pi\lambda_b \int_{r_0}^\infty u\tilde{\eta} \frac{Rb_0 s^{-2\alpha} r^{2\alpha}}{a_0 d_{\tilde{i}}} e^{-zu\tilde{\eta} \frac{Rb_0 s^{-2\alpha} r^{2\alpha}}{a_0 d_{\tilde{i}}}} ds)V(z, \frac{b_0}{a_0}))) \exp(-2\pi\lambda_e \int_{r_0}^\infty (1 - (\sum_{u=0}^U (-1)^u \binom{U}{u})V(z, \frac{b_0}{a_0}))r dr) dz \quad (30)$$

$$P_{\text{out}}^{w_1} = \int_0^\infty (1 - (\tilde{F}(\frac{(2^{\tilde{R}_1}(1+z)-1)b_1}{a_1 - \frac{(2^{\tilde{R}_1}(1+z)-1)a_0 b_1}{b_0}}))^2)(-2\pi\lambda_e(\int_{r_0}^\infty r dr(-\sum_{u=0}^U (-1)^u \binom{U}{u})(-u\tilde{\eta}(\frac{Rb_1}{a_1 d_{\tilde{i}}}-1) - 2\pi\lambda_b \int_{r_0}^\infty u\tilde{\eta} \frac{Rb_1 s^{-2\alpha} r^{2\alpha}}{a_1 d_{\tilde{i}}} e^{-zu\tilde{\eta} \frac{Rb_1 s^{-2\alpha} r^{2\alpha}}{a_1 d_{\tilde{i}}}} ds)V(z, \frac{b_1}{a_1}))) \exp(-2\pi\lambda_e \int_{r_0}^\infty (1 - (\sum_{u=0}^U (-1)^u \binom{U}{u})V(z, \frac{b_1}{a_1}))r dr) dz \quad (31)$$

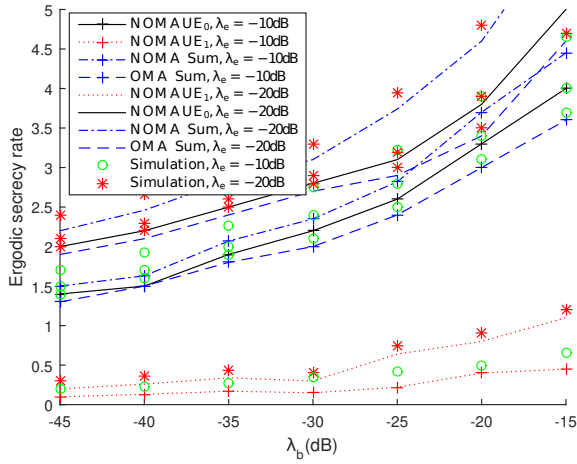


Fig. 2. Ergodic secrecy rate versus BS's density and two different  $\lambda_e$ .

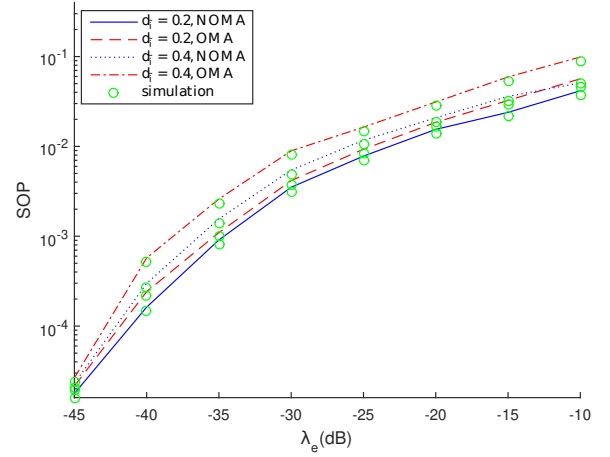


Fig. 4. SOP versus  $\lambda_e$  ( $\tilde{R}_0 = 1.5$  BPCU,  $\tilde{R}_1 = 0.5$  BPCU).

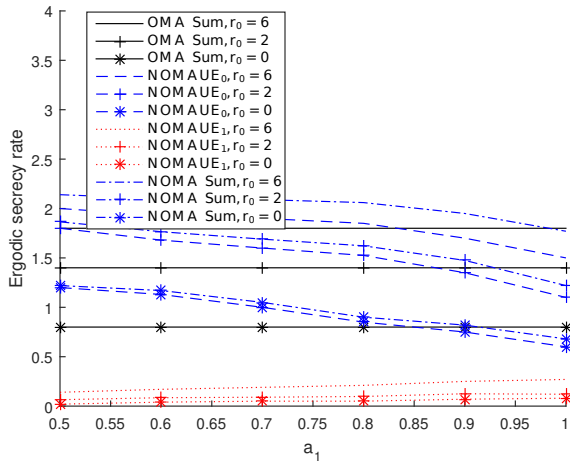


Fig. 3. Ergodic secrecy rate versus  $a_1$  and different  $r_0$ .

the secrecy rate increases; because this degrades the channel conditions for the eavesdroppers. With no eavesdropper-free region ( $r_0 = 0$ ), a positive secrecy rate is still achievable, but its value highly depends on  $\lambda_e$ .

Fig. 4 shows the total SOP as a function of  $\lambda_e$ , for two different  $d_{\tilde{i}}$  (power coefficients attackers allocate to the  $\tilde{i}$ -th pilot sequence during channel estimation phase). The density of BS is  $\lambda_b = -40$  dB and the targeted secrecy rate for the users is  $\tilde{R}_0 = 1.5$  and  $\tilde{R}_1 = 0.5$  bits per channel use (BPCU). As expected, for both NOMA and OMA, the higher  $d_{\tilde{i}}$  is, the higher SOP will be, due to the increased SINR at the attacker; which in turn leads to increased leakage. SOP increases with increasing attacker density and NOMA has better performance compared to OMA. In addition, with increasing  $d_{\tilde{i}}$ , the SOP increase for OMA is higher than that for NOMA; OMA is more sensitive to  $d_{\tilde{i}}$ , because for a given target secrecy rate,  $R_{th}$ , OMA has a multiplicative factor  $2R_{th}$  in the SINR threshold; moreover, by allocating all power to one user during one slot (half of the time), the SINR at the attacker is more sensitive to  $d_{\tilde{i}}$ .

Fig. 5 shows the SOP for the central and second users, for both NOMA and OMA, as a function of  $\lambda_b$ ; for two different target secrecy rates, and  $\lambda_e = -45$  dB. Obviously, higher target secrecy rate results in higher secrecy outage. The effect on the target secrecy rate is higher for OMA, for both central and second users, compared to NOMA, due to



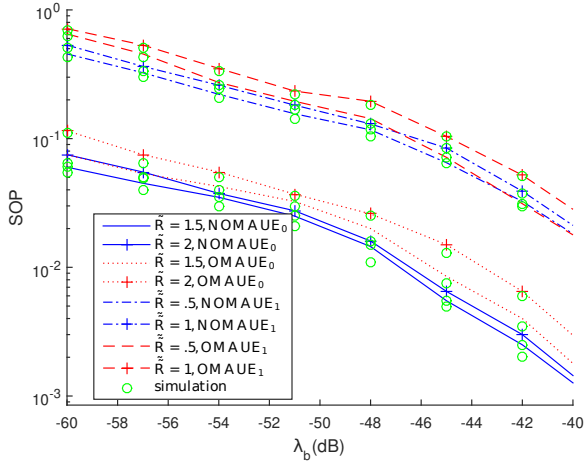


Fig. 5. SOP versus  $\lambda_b$  and two different  $\tilde{R}_0$  and  $\tilde{R}_1$ .

the multiplication factor  $2R_{th}$ . Moreover, for the high BS density, the OMA outage probability for the second user reaches a slightly smaller value than for NOMA in the low  $\tilde{R}_1$ . The reason is that the second user in NOMA experiences interference from the central user, which is not the case in OMA. But, by increasing  $\tilde{R}_1$ , the effect of multiplication factor 2 turns out to dominate and it results in a higher outage for the second OMA user.

### VIII. CONCLUSION

We analyzed the performance of physical layer security techniques for massive MIMO-NOMA networks in the presence of active attackers. Random user pairing was adopted and users were clustered, with two NOMA users in each cluster. During the channel estimation phase, the attackers send a combination of all pilot sequences. A PPP modeled random locations of nodes. We characterized a lower bound on the ergodic secrecy rate and SOP and show that NOMA provides a performance improvement over OMA, for appropriate power allocation among NOMA users.

### REFERENCES

- [1] E. G. Larsson, O. Edfors, F. Tufvesson, and T. L. Marzetta, "Massive MIMO for next generation wireless systems," *IEEE Comm. Magazine*, vol. 52, pp. 186–195, 2014.
- [2] W. Hao, M. Zeng, Z. Chu, S. Yang, and G. Sun, "Energy-efficient resource allocation for mmwave massive MIMO hetnets with wireless backhaul," *IEEE Access*, vol. PP, 2017.
- [3] J. Hoydis, S. Brink, and M. Debbah, "Massive MIMO in the ULDL of cellular networks: How many antennas do we need?," *Selected Areas in Comm., IEEE Journal on*, vol. 31, pp. 160–171, 02 2013.
- [4] O. Elijah, C. Y. Leow, T. A. Rahman, S. Nunoo, and S. Z. Iliya, "A comprehensive survey of pilot contamination in massive MIMO5g system," *IEEE Comm. Surveys Tutorials*, vol. 18, no. 2, pp. 905–923, 2016.
- [5] Z. Ding, Z. Yang, P. Fan, and H. V. Poor, "On the performance of non-orthogonal multiple access in 5g systems with randomly deployed users," *IEEE Signal Processing Letters*, vol. 21, pp. 1501–1505, Dec 2014.
- [6] K. Higuchi and A. Benjebbour, "Non-orthogonal multiple access (NOMA) with successive interference cancellation for future radio access," *IEICE Trans. on Comm.*, vol. E98.B, pp. 403–414, 03 2015.

- [7] X. Chen, Z. Zhang, C. Zhong, R. Jia, and D. W. K. Ng, "Fully non-orthogonal communication for massive access," *IEEE Trans. on Comm.*, 12 2017.
- [8] X. Chen, Z. Zhang, C. Zhong, D. W. K. Ng, and R. Jia, "Exploiting inter-user interference for secure massive non-orthogonal multiple access," *IEEE Journal on Selected Areas in Comm.*, vol. 36, pp. 788–801, April 2018.
- [9] D. Kapetanovic, G. Zheng, and F. Rusek, "Physical layer security for massive MIMO: An overview on passive eavesdropping and active attacks," *IEEE Comm. Magazine*, vol. 53, no. 6, pp. 21–27, 2015.
- [10] L. Lu, G. Y. Li, A. L. Swindlehurst, A. Ashikhmin, and R. Zhang, "An overview of massive MIMO: Benefits and challenges," *IEEE Journal of Selected Topics in Signal Processing*, vol. 8, pp. 742–758, Oct 2014.
- [11] B. Akgun, M. Krunz, and O. Ozan Koyluoglu, "Vulnerabilities of massive MIMO systems to pilot contamination attacks," *IEEE Trans. on Infor. Forensics and Security*, vol. 14, pp. 1251–1263, May 2019.
- [12] T. Bai and R. W. Heath, "Coverage and rate analysis for millimeter-wave cellular networks," *IEEE Trans. on Wireless Comm.*, vol. 14, pp. 1100–1114, Feb 2015.
- [13] Y. Zhang, H. Wang, Q. Yang, and Z. Ding, "Secrecy sum rate maximization in non-orthogonal multiple access," *IEEE Comm. Letters*, vol. 20, pp. 930–933, May 2016.
- [14] Y. Liu, Z. Qin, M. Elkashlan, Y. Gao, and L. Hanzo, "Enhancing the physical layer security of non-orthogonal multiple access in large-scale networks," *IEEE Trans. on Wireless Comm.*, vol. 16, pp. 1656–1672, March 2017.
- [15] M. Abolpour, M. Mirmohseni, and M. R. Aref, "On the secrecy performance of NOMA systems with both external and internal eavesdroppers," *ArXiv*, vol. abs/1906.03929, 2019.
- [16] J. K. Tugnait, "Self-contamination for detection of pilot contamination attack in multiple antenna systems," *IEEE Wireless Comm. Letters*, vol. 4, pp. 525–528, Oct 2015.
- [17] Y. Wu, R. Schober, D. W. K. Ng, C. Xiao, and G. Caire, "Secure massive MIMO transmission with an active eavesdropper," *IEEE Trans. on Infor. Theory*, vol. 62, pp. 3880–3900, July 2016.
- [18] S. Kusaladharma, G. Amarasinghaya, W. . Zhu, and W. Ajib, "Rate analysis for noma in massive MIMO based stochastic cellular networks with pilot contamination," in *2018 IEEE Global Comm. Conf. (GLOBECOM)*, Dec 2018.
- [19] T.-J. Huang, "Theoretical analysis of noma within massive mimo systems," *Wireless Personal Communications*, 01 2020.
- [20] L. Sanguinetti, E. Björnson, and J. Hoydis, "Toward massive mimo 2.0: Understanding spatial correlation, interference suppression, and pilot contamination," *IEEE Transactions on Communications*, vol. 68, no. 1, pp. 232–257, 2020.
- [21] F. Rusek, D. Persson, B. K. Lau, E. G. Larsson, T. L. Marzetta, O. Edfors, and F. Tufvesson, "Scaling up MIMO: Opportunities and challenges with very large arrays," *IEEE Signal Processing Magazine*, vol. 30, pp. 40–60, Jan 2013.
- [22] J. Zhu, R. Schober, and V. K. Bhargava, "Secure transmission in multicell massive MIMO systems," *IEEE Trans. on Wireless Comm.*, vol. 13, pp. 4766–4781, Sep. 2014.
- [23] M. Doherty, "Mathematical modeling. a chemical engineer's perspective by rutherford aris," *Aiche Journal - AICHE J*, vol. 48, pp. 1362–1363, 06 2002.
- [24] S. Chiu, D. Stoyan, W. Kendall, and J. Mecke, *Stochastic Geometry and Its Applications*. 2013.
- [25] Z. Yazdandshenasan, H. S. Dhillon, M. Afshang, and P. H. J. Chong, "Poisson hole process: Theory and applications to wireless networks," *IEEE Transactions on Wireless Communications*, vol. 15, no. 11, pp. 7531–7546, 2016.
- [26] C. Lee and M. Haenggi, "Interference and outage in poisson cognitive networks," *IEEE Transactions on Wireless Communications*, vol. 11, no. 4, pp. 1392–1401, 2012.

### APPENDIX A PROOF OF LEMMA 1

As the intended signal for the user in the  $\tilde{i}$ -th cluster of the  $k$ -th cell is  $s_{k0\tilde{i}}$ , by defining  $\mathcal{D} = \{(i, m) | i \in \{1, \dots, I\}, m \in \{0, 1\}\}$ , we write (10) as  $y_{k0\tilde{i}} = I_0 + I_1 + I_2 + w_d$ .  $I_0$ ,  $I_1$  and  $I_2$ , respectively, are the desired signal for the central user, the interference caused by the second user in the same cell, and



the interference caused by the users in other cells, which are calculated in (32). We have  $\text{SINR}_{k0\tilde{i}}^{w_0} = \frac{E[I_0^2]}{E[Y_{k0\tilde{i}}]}$ . We apply the massive MIMO condition,  $M \rightarrow \infty$ , and compute  $\text{SINR}_{k0\tilde{i}}^{w_0}$  in this regime. According to (3) and (5), in  $I_0$  only  $\mathbf{h}_{kk0\tilde{i}}^H \mathbf{h}_{kk0\tilde{i}}$  is proportional to  $M$  and the other terms tend to zero. In  $I_1$ , all terms tend to zero (the term including  $\sqrt{a_1} s_{k1\tilde{i}}$  will be zero because of applying SIC at the central user), and in (32) only  $\mathbf{h}_{lk0\tilde{i}}^H \mathbf{h}_{lk0\tilde{i}}$  will be a non-vanishing term. Therefore, for  $M \rightarrow \infty$ , we have:

$$\text{SINR}_{k0\tilde{i}}^{w_0} = \frac{\frac{M P_d a_0 r_{kk0\tilde{i}}^{-2\alpha}}{2}}{\sigma_n^2 + \frac{M P_d b_0}{2} \sum_{l \neq k} r_{lk0\tilde{i}}^{-2\alpha} \left( \sum_{m=0}^1 \frac{a_m}{b_m} \right)}. \quad (33)$$

In addition, when  $M \rightarrow \infty$ ,  $\sigma_n^2$  is negligible in comparison with other terms; thus, by defining  $R \triangleq \sum_{m=0}^1 \frac{a_m}{b_m}$  we obtain:

$$\text{SINR}_{k0\tilde{i}}^{w_0} = \frac{a_0 r_{kk0\tilde{i}}^{-2\alpha}}{R b_0 \sum_{l \neq k} r_{lk0\tilde{i}}^{-2\alpha}}. \quad (34)$$

Following similar steps,  $\text{SINR}_{k0\tilde{i}}^{w_1}$  and  $\text{SINR}_{k1\tilde{i}}^{w_1}$  in the massive MIMO regimes are calculated. This completes the proof.

#### APPENDIX B PROOF OF LEMMA 2

First, we show that the central user is able to perform SIC. To show this, we must check if  $\text{SINR}_{k0\tilde{i}}^{w_1} > \text{SINR}_{k1\tilde{i}}^{w_1}$ . Using (12) and (13) and after some simple mathematical manipulations, we obtain  $\frac{r_{kk0\tilde{i}}^{-2\alpha}}{\sum_{l \neq k} r_{lk0\tilde{i}}^{-2\alpha}} > \frac{r_{kk1\tilde{i}}^{-2\alpha}}{\sum_{l \neq k} r_{lk1\tilde{i}}^{-2\alpha}}$  which is realized by the definition of central and second users mentioned in Subsection IV-B. Thus, the central user is able to perform SIC. By defining  $S_0 = \frac{r_{kk0\tilde{i}}^{-2\alpha}}{\sum_{l \neq k} r_{lk0\tilde{i}}^{-2\alpha}}$  and  $2^t - 1 = T$ , we have:

$$\begin{aligned} R_0 &= E[\log(1 + \text{SINR}_{k0\tilde{i}}^{w_0})] = \int_0^\infty P(\log(1 + \text{SINR}_{k0\tilde{i}}^{w_0}) > t) dt \\ &= \int_0^\infty P\left(\frac{a_0 r_{kk0\tilde{i}}^{-2\alpha}}{R b_0 \sum_{l \neq k} r_{lk0\tilde{i}}^{-2\alpha}} > 2^t - 1\right) dt \\ &= \int_0^\infty (1 - F_{S_0}\left(\frac{T R b_0}{a_0}\right)) dt. \end{aligned} \quad (35)$$

Moreover, by defining  $S_1 = \frac{r_{kk1\tilde{i}}^{-2\alpha}}{\sum_{l \neq k} r_{lk1\tilde{i}}^{-2\alpha}}$ , the ergodic rate of the second user is:

$$\begin{aligned} R_1 &= E[\log(1 + \text{SINR}_{k1\tilde{i}}^{w_1})] = \int_0^\infty P(\text{SINR}_{k1\tilde{i}}^{w_1} > 2^t - 1) dt \\ &= \int_0^\infty P\left(\frac{a_1 r_{kk1\tilde{i}}^{-2\alpha}}{\frac{a_0 b_1 r_{kk1\tilde{i}}^{-2\alpha}}{b_0} + R b_1 \sum_{l \neq k} r_{lk1\tilde{i}}^{-2\alpha}} > 2^t - 1\right) dt \\ &\stackrel{(a)}{=} \int_0^{\log \frac{a_1 b_0}{a_0 b_1} + 1} (1 - F_{S_1}\left(\frac{T R b_1}{a_1 - \frac{T a_0 b_1}{b_0}}\right)) dt, \end{aligned} \quad (36)$$

where (a) is due to:

$$\lim_{\sum_{l \neq k} r_{lk1\tilde{i}}^{-2\alpha} \rightarrow 0} \left( \frac{a_1 r_{kk1\tilde{i}}^{-2\alpha}}{\frac{a_0 b_1 r_{kk1\tilde{i}}^{-2\alpha}}{b_0} + R b_1 \sum_{l \neq k} r_{lk1\tilde{i}}^{-2\alpha}} \right) = \frac{a_1 b_0}{a_0 b_1}. \text{ So, we need}$$

to calculate the CDF of  $S = \frac{r_{kk\tilde{i}}^{-2\alpha}}{\sum_{l \neq k} r_{lk\tilde{i}}^{-2\alpha}}$ , where  $r_{kk\tilde{i}}$  and  $r_{lk\tilde{i}}$  are distances between a randomly selected user in  $\tilde{i}$ -th cluster of  $k$ -th cell and its serving BS and interfering BSs, respectively. Now, we use order statistics to compute the CDF of  $S_0 = \max(S_0, S_1)$  and  $S_1 = \min(S_0, S_1)$ , as follows:

$$\begin{aligned} F_{S_1}(s_1) &= 2F_S(s_1) - F_S^2(s_1), \\ F_{S_0}(s_0) &= F_S^2(s_0). \end{aligned} \quad (37)$$

The CDF of  $S$  is calculated as:

$$\begin{aligned} F_S(s) &= 1 - E_{r_{kk\tilde{i}}} [P(S > s) | r_{kk\tilde{i}} = r] \\ &= 1 - \int_0^\infty P\left(\frac{r_{kk\tilde{i}}^{-2\alpha}}{\sum_{l \neq k} r_{lk\tilde{i}}^{-2\alpha}} > s | r_{kk\tilde{i}} = r\right) f_{r_{kk\tilde{i}}}(r) dr, \end{aligned} \quad (38)$$

As each user connects to its nearest BS, no BS must be in a disk of radius  $r$ . So we have:

$$\begin{aligned} P(r_{kk\tilde{i}} > r) &= e^{-\lambda_b \pi r^2} = 1 - F_{r_{kk\tilde{i}}}(r), \\ f_{r_{kk\tilde{i}}}(r) &= 2\pi \lambda_b r e^{-\lambda_b \pi r^2}. \end{aligned} \quad (39)$$

Now, we have:

$$\begin{aligned} P\left(\frac{r_{kk\tilde{i}}^{-2\alpha}}{\sum_{l \neq k} r_{lk\tilde{i}}^{-2\alpha}} > s | r_{kk\tilde{i}} = r\right) &= P\left(1 > s \left(\frac{\sum_{l \neq k} r_{lk\tilde{i}}^{-2\alpha}}{r^{-2\alpha}}\right)\right) \\ &\stackrel{(a)}{\cong} P(g > s \left(\frac{\sum_{l \neq k} r_{lk\tilde{i}}^{-2\alpha}}{r^{-2\alpha}}\right)) \\ &\stackrel{(b)}{=} P(g > sA) = 1 - \int P(g < sA | A = a) f_A(a) da \\ &= 1 - E_A[F_g(sA)] \stackrel{(c)}{=} \sum_{n=1}^N (-1)^{n+1} \binom{N}{n} E[e^{-s^n \eta A}], \end{aligned} \quad (40)$$

(a) follows from the fact that we approximate 1 with a dummy Gamma random variable,  $g$ , with unit mean and the shape parameter of  $N$  such that [23]:

$$\lim_{N \rightarrow \infty} \frac{N^N g^{N-1} e^{-Ng}}{\Gamma(N)} = \delta(g-1), \quad (41)$$

where  $\delta(\cdot)$  is the Dirac delta function and  $\Gamma(\cdot)$  is the Gamma function defined as  $\Gamma(a) = \int_0^\infty e^{-t} t^{a-1} dt$ . (b) follows from defining  $A \triangleq \frac{\sum_{l \neq k} r_{lk\tilde{i}}^{-2\alpha}}{r^{-2\alpha}}$ . (c) follows from the fact that we use the Alzer inequality in [12, Appendix A] to give a tight approximation of the CDF, as  $F_g(A) = (1 - e^{-AN(N!)^{\frac{1}{N}}})^N$ ; then we use a binary extension, defining  $\eta = N(N!)^{\frac{1}{N}}$ . Moreover, we have:

$$\begin{aligned} E[e^{-s^n \eta A}] &= E[e^{-\eta n s r^{2\alpha} \sum_{l \neq k} r_{lk\tilde{i}}^{-2\alpha}}] \\ &\stackrel{(a)}{=} \int_r [\exp(-\eta n s x^{-2\alpha} r^{2\alpha}) - 1] 2\pi \lambda_b x dx, \end{aligned} \quad (42)$$

where (a) is due to the probability generating functional (PGFL) of the PPP [24] and the fact that distances from other

$$\begin{aligned}
I_0 &= r_{kk0\bar{i}}^{-\alpha/2} s_{k0\bar{i}} \sqrt{\frac{P_d a_0}{2M}} (\mathbf{h}_{kk0\bar{i}}^H \mathbf{h}_{kk0\bar{i}} r_{kk0\bar{i}}^{-\alpha/2} + \sum_{\mathcal{B} \setminus \{s=0, t=k\}} \frac{\mathbf{h}_{kk0\bar{i}}^H \mathbf{h}_{kts\bar{i}} r_{kts\bar{i}}^{-\alpha/2} \sqrt{b_s}}{\sqrt{b_0}} + \sum_{e \in \phi_e} \frac{\mathbf{h}_{kk0\bar{i}}^H \mathbf{g}_{ke} r_{ke}^{-\alpha/2} \sqrt{d_{\bar{i}}}}{\sqrt{b_0}} + \frac{\mathbf{h}_{kk0\bar{i}}^H \mathbf{W}_k \boldsymbol{\varphi}_{\bar{i}}^*}{\sqrt{b_0 P_p}}), \\
I_1 &= r_{kk0\bar{i}}^{-\alpha/2} \sum_{\mathcal{D} \setminus \{i=\bar{i}, m=0\}} s_{kmi} \sqrt{\frac{P_d a_m}{2M}} (\mathbf{h}_{kk0\bar{i}}^H \mathbf{h}_{kkmi} r_{kkmi}^{-\alpha/2} + \sum_{\mathcal{B} \setminus \{s=m, t=k\}} \frac{\mathbf{h}_{kk0\bar{i}}^H \mathbf{h}_{ktsi} r_{ktsi}^{-\alpha/2} \sqrt{b_s}}{\sqrt{b_m}} + \sum_{e \in \phi_e} \frac{\mathbf{h}_{kk0\bar{i}}^H \mathbf{g}_{ke} r_{ke}^{-\alpha/2} \sqrt{d_{\bar{i}}}}{\sqrt{b_m}} \\
&\quad + \frac{\mathbf{h}_{kk0\bar{i}}^H \mathbf{W}_k \boldsymbol{\varphi}_{\bar{i}}^*}{\sqrt{b_m P_p}}), \\
I_2 &= \sum_{l \neq k} r_{lk0\bar{i}}^{-\alpha/2} \sum_{i=1}^I \sum_{m=0}^1 s_{lmi} \sqrt{\frac{P_d a_m}{2M}} (\mathbf{h}_{lk0\bar{i}}^H \mathbf{h}_{llmi} r_{llmi}^{-\alpha/2} + \sum_{\mathcal{B} \setminus \{s=m, t=l\}} \frac{\mathbf{h}_{lk0\bar{i}}^H \mathbf{h}_{ltsi} r_{ltsi}^{-\alpha/2} \sqrt{b_s}}{\sqrt{b_m}} + \sum_{e \in \phi_e} \frac{\mathbf{h}_{lk0\bar{i}}^H \mathbf{g}_{le} r_{le}^{-\alpha/2} \sqrt{d_{\bar{i}}}}{\sqrt{b_m}} \\
&\quad + \frac{\mathbf{h}_{lk0\bar{i}}^H \mathbf{W}_l \boldsymbol{\varphi}_{\bar{i}}^*}{\sqrt{b_m P_p}}). \tag{32}
\end{aligned}$$

BSs to the user must be larger than  $r_{kk\bar{i}}$ . So, by combining (40) and (42), we have:

$$\begin{aligned}
P\left(\frac{r_{kk\bar{i}}^{-2\alpha}}{\sum_{l \neq k} r_{lk\bar{i}}^{-2\alpha}} > s \mid r_{kk\bar{i}} = r\right) \\
= \sum_{n=1}^N (-1)^{n+1} \binom{N}{n} e^{\int_r [\exp(-s\eta n r^{2\alpha} x^{-2\alpha}) - 1] 2\pi\lambda_b x dx}. \tag{43}
\end{aligned}$$

By replacing (43) and (39) into (38), the CDF of  $S$  is:

$$\begin{aligned}
F_S(s) = 1 - \int_0^\infty \sum_{n=1}^N (-1)^{n+1} \binom{N}{n} \\
e^{\int_r [\exp(-s\eta n r^{2\alpha} x^{-2\alpha}) - 1] 2\pi\lambda_b x dx} 2\pi\lambda_b r e^{-\lambda_b \pi r^2} dr. \tag{44}
\end{aligned}$$

Finally, by substituting (44) into (37), (35) and (36) are calculated.

### APPENDIX C PROOF OF LEMMA 3

The location of the attackers follow a Poisson hole process (PHP) [25] with  $\phi_e$  as the *baseline* PPP from which the holes (disks of radius  $r_0$  around BS), represented by  $\phi_b$  (the center of the holes), are carved out. Due to the impossibility of analyzing the exact overlap among holes, the PGFL of a PHP is unknown and one approach to circumvent this problem is ignoring the effect of holes and approximating the PHP by the *baseline* PPP [26]. This leads to overestimating the interference caused by attackers. To minimize the number of probable attackers that fall into the holes, we assume that  $r_0$  is much smaller than the mean nearest-neighbor distance of  $\phi_b$  which, according to (38), has a Rayleigh distribution with parameter  $(\sqrt{2\pi\lambda_b})^{(-1)}$  and mean  $(\sqrt{2\pi\lambda_b})^{(-1)} \sqrt{\frac{\pi}{2}}$ . So, the area covered by the holes is much smaller than the total region

of the network.

According to statistical properties, we have:

$$E[\log(1 + \text{SINR}_{\bar{e}}^{w_0})] = \frac{1}{\ln 2} \int_0^\infty \frac{1 - F_{\text{SINR}_{\bar{e}}^{w_0}}(x)}{1+x} dx. \tag{45}$$

By considering the attacker with best channel condition (i.e., worst case scenario), using (15) and defining  $I = \sum_{l \neq k} r_{l\bar{e}}^{-2\alpha}$ , we obtain:

$$\begin{aligned}
F_{\text{SINR}_{\bar{e}}^{w_0}}(x) &= P(\text{SINR}_{\bar{e}}^{w_0} < x) \\
&= P\left(\max_{\bar{e} \in \phi_e} \frac{\frac{d_{\bar{i}} a_0 r_{k\bar{e}}^{-2\alpha}}{b_0}}{r_{k\bar{e}}^{-2\alpha} (R - \frac{d_{\bar{i}} a_0}{b_0}) + R \sum_{l \neq k} r_{l\bar{e}}^{-2\alpha}} < x\right) \\
&\stackrel{(a)}{=} E_{\phi_e} \left[ \prod_{\bar{e} \in \phi_e} P\left(\frac{\frac{d_{\bar{i}} a_0 r_{k\bar{e}}^{-2\alpha}}{b_0}}{r_{k\bar{e}}^{-2\alpha} (R - \frac{d_{\bar{i}} a_0}{b_0}) + RI} < x \mid \phi_e\right) \right] \\
&\stackrel{(b)}{=} \exp(-2\pi\lambda_e \int_{r_0}^\infty (1 - P(\frac{\frac{d_{\bar{i}} a_0 r^{-2\alpha}}{b_0}}{r^{-2\alpha} (R - \frac{d_{\bar{i}} a_0}{b_0}) + RI} < x)) r dr. \tag{46}
\end{aligned}$$

where (a) is due to maximum statistical property and (b) is due to the PGFL of the PPP and the fact that  $r_0$  is the radius of eavesdropper-free zone. Now, we calculate  $P(\frac{\frac{d_{\bar{i}} a_0 r^{-2\alpha}}{b_0}}{r^{-2\alpha} (R - \frac{d_{\bar{i}} a_0}{b_0}) + RI} < x)$ . Let,  $\frac{\frac{d_{\bar{i}} a_0 r^{-2\alpha}}{b_0}}{r^{-2\alpha} (R - \frac{d_{\bar{i}} a_0}{b_0}) + RI} \triangleq \text{SINR}$ . We have:

$$P(\text{SINR} < x) = P(1 < x \text{SINR}^{-1}) \stackrel{(a)}{\approx} P(g < x \text{SINR}^{-1}), \tag{47}$$

where  $g$  is a dummy Gamma random variable with unit mean and shape parameter  $U$ . Also (41) holds by replacing  $N$  by  $U$ . Now, by defining  $\tilde{\eta} = U(U!)^{\frac{1}{U}}$ , (47) will be:

$$\begin{aligned}
P(\text{SINR} < x) &\stackrel{(a)}{=} E[(1 - e^{-x \text{SINR}^{-1} \tilde{\eta}})^U] \\
&\stackrel{(b)}{=} \sum_{u=0}^U (-1)^u \binom{U}{u} E[e^{-xu \tilde{\eta} \text{SINR}^{-1}}], \tag{48}
\end{aligned}$$

where (a) and (b) result from an approach similar to (40)-(c). We obtain:

$$E[e^{-xu\tilde{\eta}\text{SINR}^{-1}}] = E[e^{-xu\tilde{\eta}(\frac{Rb_0}{a_0d_i} - 1)} e^{-xu\tilde{\eta}\frac{Rb_0r^{2\alpha}}{a_0d_i} \sum_{l \neq k} r_l^{-2\alpha}}] \\ \stackrel{(a)}{=} e^{-xu\tilde{\eta}(\frac{Rb_0}{a_0d_i} - 1)} \exp(-2\pi\lambda_b \int_{r_0}^{\infty} (1 - e^{-xu\tilde{\eta}\frac{Rb_0s^{-2\alpha}r^{2\alpha}}{a_0d_i}}) s ds). \quad (49)$$

where (a) is obtained by the PGFL of the PPP and using the fact that by conditioning on the distance between the attacker and the serving BS in the  $k$ -th cell, the point process of other BSs, i.e.,  $\phi_b \setminus k$ , follows a reduced Palm distribution of the PPP where by the use of Slivnyak-Mecke theorem is the same as the original PPP [24]. In brief, first we condition the event on the attacker location. Then we average over BS locations, thus we see the BS density in (49)-(a). Finally, By combining (45), (46), (48) and (49), the ergodic leakage rate to the attacker is shown by (23) to complete the proof.

#### APPENDIX D PROOF OF LEMMA 4

$P_{\text{out}}^{w_0}$  is calculated as follows:

$$P_{\text{out}}^{w_0} = P(\log(1 + \text{SINR}_{k0\tilde{i}}^{w_0}) - \log(1 + \text{SINR}_{\tilde{e}}^{w_0}) < \tilde{R}_0) \\ \stackrel{(a)}{=} \int_0^{\infty} P(\text{SINR}_{k0\tilde{i}}^{w_0} < 2^{\tilde{R}_0}(1+z) - 1) f_{\text{SINR}_{\tilde{e}}^{w_0}}(z) dz, \quad (50)$$

(a) is obtained by conditioning on the attacker SINR. First, we compute the inner term in (50)-(a):

$$P(\text{SINR}_{k0\tilde{i}}^{w_0} < 2^{\tilde{R}_0}(1+z) - 1) = F_{S_0}(\frac{Rb_0(2^{\tilde{R}_0}(1+z) - 1)}{a_0}), \quad (51)$$

(51) can be obtained by substituting (44) into (37) and replacing  $s$  by  $\frac{Rb_0(2^{\tilde{R}_0}(1+z)-1)}{a_0}$ . Moreover, according to (45) and (23), we have:

$$F_{\text{SINR}_{\tilde{e}}^{w_0}}(x) = \exp(-2\pi\lambda_e \int_{r_0}^{\infty} (1 - (\sum_{u=0}^U (-1)^u \binom{U}{u}) \{e^{-xu\tilde{\eta}(\frac{Rb_0}{a_0d_i} - 1)} \exp(-2\pi\lambda_b \int_{r_0}^{\infty} (1 - e^{-xu\tilde{\eta}\frac{Rb_0s^{-2\alpha}r^{2\alpha}}{a_0d_i}}) s ds)\}) r dr). \quad (52)$$

So,  $f_{\text{SINR}_{\tilde{e}}^{w_0}}$  is calculated by taking the derivative with respect to  $x$ . Finally,  $P_{\text{out}}^{w_0}$  is calculated as shown in (30). Moreover,  $P_{\text{out}}^{w_1}$  is calculated as follows:

$$P_{\text{out}}^{w_1} = P(\log(1 + \text{SINR}_{k1\tilde{i}}^{w_1}) - \log(1 + \text{SINR}_{\tilde{e}}^{w_1}) < \tilde{R}_1) \\ = \int_0^{\infty} P(\text{SINR}_{k1\tilde{i}}^{w_1} < 2^{\tilde{R}_1}(1+z) - 1) f_{\text{SINR}_{\tilde{e}}^{w_1}}(z) dz. \quad (53)$$

In addition, we have:

$$P(\text{SINR}_{k1\tilde{i}}^{w_1} < 2^{\tilde{R}_1}(1+z) - 1) = F_{S_1}(\frac{(2^{\tilde{R}_1}(1+z) - 1)Rb_1}{a_1 - \frac{(2^{\tilde{R}_1}(1+z)-1)a_0b_1}{b_0}}), \quad (54)$$

where (54) can be found by substituting (44) into (37) and replacing  $s$  by  $\frac{(2^{\tilde{R}_1}(1+z)-1)Rb_1}{a_1 - \frac{(2^{\tilde{R}_1}(1+z)-1)a_0b_1}{b_0}}$ . Also, from (15) and (16), it is obvious that  $F_{\text{SINR}_{\tilde{e}}^{w_1}}(x)$  can be computed by replacing  $a_0$  and  $b_0$  in  $F_{\text{SINR}_{\tilde{e}}^{w_0}}(x)$ , with  $a_1$  and  $b_1$  respectively. So we can compute  $f_{\text{SINR}_{\tilde{e}}^{w_1}}(x)$  and by substituting it and (54) into (53),  $P_{\text{out}}^{w_1}$  is computed as (31).